

# Bicriterion optimisation for traction substations in mass rapid transit systems using genetic algorithm

C.S.Chang  
W.Wang  
A.C.Liew  
F.S.Wen

Indexing terms: Load sharing, Optimisation problems, Power recovery, Regenerative braking, Mass rapid transit system

**Abstract:** In modern mass rapid transit systems trains are often equipped with regenerative braking. Effective control of firing angles at traction substations (TSS) will bring about high recovery of regenerated power, even load sharing among TSS and thus economic returns. These two objectives of high power recovery and even load sharing are conflicting, and do not reach their optima simultaneously. A tradeoff approach is proposed for optimising these two objectives and for compromising with other objectives using a genetic algorithm. Consistent power saving has been obtained from optimisation results and load sharing can be greatly improved through co-ordinated optimisation of TSS firing angles. The optimisation presented is carried out at a particular 'snap shot'. The proposed approach is being extended to a time period for dealing with overall energy recovery.

## List of principal symbols

$N$	Number of railway elements
$Obj1(\bar{\beta})$	First objective function
$Obj2(\bar{\beta})$	Second objective function
$P, Q$	Active and reactive power
$Fit(\bar{\beta})$	Fitness function
$V_d$	DC busbar voltage
$I_d$	DC busbar injected current
$G$	DC system conductance matrix
$a$	Transformer off-nominal turns ratio
$MG$	Maximum number of generations
$N_p$	Population in each generation
$\beta$	Traction substation firing angle
$\rho$	Objective weight
$\phi$	Power factor angle
Subscripts	
$TSS$	Traction substation
$Tr$	Train

© IEE, 1998

IEE Proceedings online no. 19981485

Paper first received 7th October 1996 and in revised form 3rd June 1997

The authors are with the Department of Electrical Engineering, National University of Singapore, 10 Kent Ridge Crescent, Singapore 119260

## 1 Introduction

Cost effectiveness is of important concern in modern MRT operation and there is a great incentive to save capital and running costs. In MRT systems trains are often equipped with regenerative and rheostatic braking [1–8]. During regenerative braking, the released power is either used by nearby trains or returned to the power supply system through traction substations (TSSs) equipped with inverters [2–6]. There is a tendency for nearby voltages to rise during the process, which could limit the amount of power recovered by these two means. Rheostatic braking is activated to prevent excessive voltages and to minimise damage to railway equipment. To ensure power recovery efficiency, rheostatic braking is avoided wherever possible to maximise power delivery.

Power recovery efficiency is usually represented by a performance index known as line receptivity. It is time-varying and depends on the direct voltage profile which is a function of train positions and power demands. Train positions and power demands are functions of the service schedule, particularly the headway and synchronous delays which vary with the period of the day [2, 3]. Line receptivity also depends on the AC supply loading conditions and the configuration of the railway supply network, such as TSS positions and other parameters.

Apart from supply configuration and service schedule, line receptivity is influenced by electrical control of TSSs, their firing angles and transformer tap positions. A fuzzy-dwell-time controller was proposed for each train [6] and is shown to be able to optimise power recovery and regularity under different TSS firing angles. Because of the time-varying system structure under different operating conditions, rheostatic loss during regenerative braking does not remain constant. Thus each TSS firing angle must be optimised dynamically in order to achieve the full power recovery for all operating conditions. This is one of the two objectives this paper addresses.

The other objective is to achieve even load sharing among TSSs. Generally, in the absence of control, the bulk of recovered power from trains is returned to the power system through nearby TSSs. Thus, power handled by these nearby TSSs will be large, and sometimes can exceed their capacities. Overall supply capacity of the railway system is thus curtailed. On the other hand, if the recovered power can be returned through all TSSs evenly, the power handled by each TSS is

decreased [9]. To achieve this it is necessary to appropriately adjust all TSS firing angles.

The two objectives are thus related to TSS firing angle control. They are conflicting and do not reach their optima simultaneously. Thus, a tradeoff must be made as a compromise between the two objectives, where an optimal solution is obtained from a problem of bicriterion railway optimisation.

Genetic algorithms (GAs) represent a general optimisation method which requires little knowledge about the problem to be optimised other than the cost of each candidate solution or its fitness function. In recent years the application of GAs to power systems has become an active research area and many papers have been published. GA is a powerful tool for solving very difficult optimisation problems with multiple, discontinuous and convex objective functions. This paper shows that GA is also suitable for solving bicriterion railway optimisation problems.

## 2 Bicriterion optimisation problem

As stated in Section 1 the two objectives of high power recovery and even load sharing are important issues of railway operation. When aspects of both objectives are considered, the railway optimisation problem becomes bicriterion. The two objectives and feasibility and quality considerations are as follows:

(a) Total power objective  $Obj1(\bar{\beta})$  is to minimise the total power for running a given set of train schedules.  $Obj1(\bar{\beta})$  measures how much the objective is achieved

$$Obj1(\bar{\beta}) = \sum_{k=1}^{N_{TSS}} P_{TSS_k}(\bar{\beta})$$

$$\bar{\beta} = (\beta_1, \beta_2, \dots, \beta_{N_{TSS}}) \quad (1)$$

where  $N_{TSS}$  is the number of TSSs.  $\beta_k$  is the firing angle of the  $k$ th TSS.

(b) Power sharing objective  $Obj2(\bar{\beta})$  measures the load sharing among TSSs, by minimising the difference between each TSS load and the average load for all the TSS

$$Obj2(\bar{\beta}) = \sum_{k=1}^{N_{TSS}} \left| P_{TSS_k}(\bar{\beta}) - \frac{\sum_{j=1}^{N_{TSS}} P_{TSS_j}(\bar{\beta})}{N_{TSS}} \right| \quad (2)$$

(c) Feasibility and quality considerations are taken to maximise the feasibility and quality of train service so as to best meet passenger satisfaction. These may be expressed in terms of fuzzy performance indices [6] in terms of

- quality of passenger service
- traffic and signalling requirements
- regularity
- electrical loading

The last consideration is reflected by the voltage profile and the degree of overloading in the railway network.

(d) Basis for solving the problem: From the objectives the problem of railway optimisation is to find the loadings of each TSS and the corresponding firing angles subject to the feasibility and quality constraints as in (c). However, objectives (a) and (b) are conflicting in that the minimum overall railway load does not always

result in the most even load sharing or *vice versa*. To account for considerations (c) in the optimisation, the types of constraints, which are sensitive to each TSS firing angle, are incorporated directly into the optimisation. Other considerations, such as passenger comfort level, are considered after the railway optimisation to ensure overall computational efficiency. Instead of including these considerations at the outset, a compromise between objectives (a) and (b) is first formed on a tradeoff curve with all railway network constraints included. All other considerations are then investigated for an overall compromise at each point of the tradeoff curve, and from which the most appropriate railway operational strategy can be determined.

### 2.1 Bicriterion global optimisation approach

The overall power recovery and load sharing are each expressed in the same unit in MW. They are then combined linearly to form a single objective for the purpose of optimisation. By a suitable optimisation process the relationship or compromise between the two objectives is first established in the form of a tradeoff function. The combined single objective function [10] has the form

$$Obj(\bar{\beta}) = \rho \cdot Obj1(\bar{\beta}) + (1 - \rho) \cdot Obj2(\bar{\beta}) \quad (3)$$

which is minimised subject to

$$V_{Tr_j}^{\min} \leq V_{Tr_j} \leq V_{Tr_j}^{\max} \quad j = 1, 2, \dots, N_{Tr} \quad (4)$$

$$V_{TSS_k}^{\min} \leq V_{TSS_k} \leq V_{TSS_k}^{\max} \quad k = 1, 2, \dots, N_{TSS} \quad (5)$$

$$\beta_k^{\min} \leq \beta_k \leq \beta_k^{\max} \quad (6)$$

where  $\rho$  is the objective weight.  $V$  and  $P$  denote the voltage and active power, respectively. Eqns. 4-6 are railway network constraints to be directly included in the optimisation.  $N_{Tr}$  is the number of trains.

Nonelectrical feasibility and quality considerations are not included in the optimisation for reasons given in subsections (c) and (d).  $Obj1(\bar{\beta})$  and  $Obj2(\bar{\beta})$  have been defined in eqns. 1 and 2, respectively. Values of  $\rho$  ranging between 0 and 1 indicate the relative significance between the two objectives. When  $\rho = 0$ , only the power sharing objective is considered and when  $\rho = 1$ , only the total power objective is accounted for.

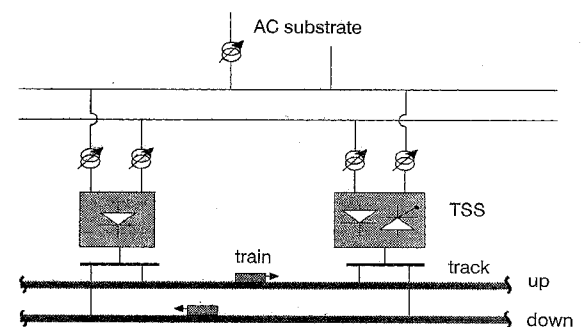


Fig. 1 Typical electrified railway network

## 3 Simulation of electrified railway operation

A typical MRT system consists of AC substations, TSSs (with or without inverter) and other components such as trains, tracks, passenger stations, and control and signalling systems (Fig. 1). Object-oriented technology [11] is applied to electrified railway simulation. The three modules (Fig. 2) in the simulation algorithm are: (a) railway operation module

that simulates effects and events occurring during railway control involving elements such as trains, tracks, and passenger stations; (b) power supply module that simulates operation of AC substations and TSSs; and (c) AC/DC loadflow module that gives the current electrical status of railway operation.

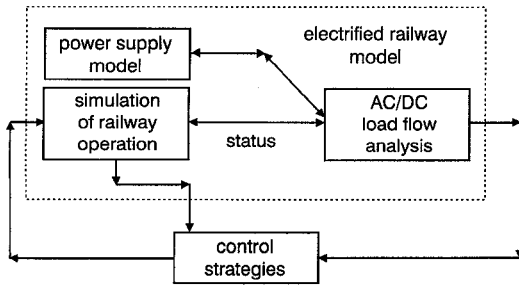


Fig. 2 Modules of railway control/simulation

### 3.1 Characteristics of MRT network configurations

MRT systems have the following electrical characteristics:

- Continuous variations of train movement and power. Train movement and power required vary with time. Trains consume or regenerate power, while they are motoring or under regenerative braking.

- Large voltage variations. In typical electrified railway networks, voltages can vary by +20 to -30% from nominal. In other power supply networks, permitted variations are generally within the  $\pm 10\%$  range.

- Nonlinear mathematical models. Railway components such as rectifiers and inverters are nonlinear elements. Mathematical models, which describe train operation are also nonlinear.

- Many railway network constraints. These include upper and lower voltage limits on each TSS and on each train, constraints on each TSS capacity, constraints on harmonic contents produced by each inverter, and constraints on power factors.

These features must be handled by a flexible and robust optimisation procedure, which has capabilities beyond those of conventional methods. GAs are suitable for solving this problem.

### 3.2 Train movement simulation

The simulation makes the following assumptions [6, 12]:

- The power consumption of each train is assumed to be dependent solely on its position.

- Likewise, the speed of each train is a sole function of its position.

- The relationship between train power consumption and its position is obtained from prior simulations of train dynamics [12].

- Fig. 3 describes regions of train operation as modelled in this paper. At low velocities, motoring torque is restricted by the armature current, since excessive current causes overheating and reduces the motor lifetime. At high velocities, motoring torque is limited by the motor power rating. Operating the motor beyond its speed limit may result in excessive stress to mechanical parts.

The traction motor model is broadly described by four regions of operation: during motoring, constant-current

characteristic at low velocities and constant-power characteristic at high velocities; and during braking, regenerative braking under normal system voltages and regenerative/rheostatic braking under excessive system voltages. Mechanical braking is applied only when electrical braking does not meet the braking requirements during emergency or when the train is approaching a stopover position. Mechanical braking is discouraged since it causes frequent maintenance and wastage of energy. Traction motor characteristics, as modelled in this paper, are thus highly nonlinear and system dependent. Modelling of these characteristics is explained in Section 3.3.

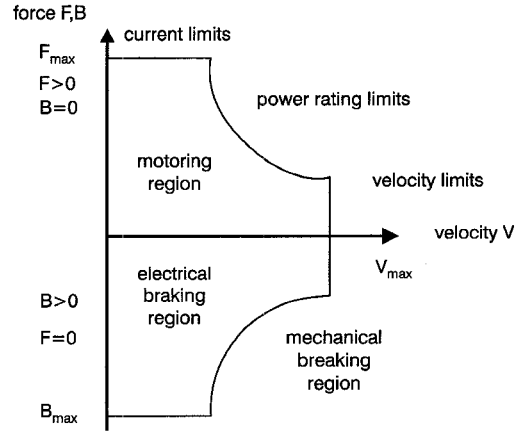


Fig. 3 Regions of train operation

Considering these conditions, the running characteristics of each train and its consumed/regenerated power are obtained from an embedded database created from prior simulations. During optimisation AC/DC loadflow is run to evaluate the current operating state, such as the voltage, power flow and line receptivity at any point of the railway system. Each operating state is related to TSS firing angles to be controlled.

### 3.3 Railway network modelling and solution

Mathematical models [2–8], corresponding to the rectifying mode and inverting mode, are implemented for each TSS. For the rectifying mode, the model is

$$V_r = V_{r0} \cos \beta_r - R_r I_r \quad (7)$$

where  $V_r$ ,  $V_{r0}$ ,  $\beta_r$ ,  $R_r$ ,  $I_r$  are, respectively, the terminal voltage, no-load voltage, firing angle, equivalent internal resistance, and current of the rectifier. For the inverting mode, the model is

$$V_i = V_{i0} \cos \beta_i - R_i I_i \quad (8)$$

where  $V_i$ ,  $V_{i0}$ ,  $\beta_i$ ,  $R_i$ ,  $I_i$  are similar to those in the model except that they refer to the inverter. Power flows in each TSS and in each train depend on the rectifier and inverter firing angles, which are obtained from AC/DC loadflow. The basic loadflow algorithm was developed by the authors [6], and is summarised in the Appendix (Section 8.1). Some modifications have been made to the algorithm to model the four regions of train operation.

## 4 Genetic algorithm and its implementation

A GA is a search procedure for modelling the mechanism of genetic evolution and natural selection [13, 14], which evolves solutions to a problem through selection, breeding and genetic variations. This procedure involves randomly generating a population

of solutions, measuring their suitability or fitness, selecting better solutions for breeding which produces a new population. The procedure is repeated to guide a highly exploitative search through a coding of parameter space, and gradually the population evolves towards the optimal solution. GAs are based on the heuristic assumptions that the best solutions will be found in regions of the parameter space containing a relatively high proportion of good solutions and that these regions can be explored by genetic operators of selection, crossover, and mutation. The power of GAs comes from the fact that they are robust and can deal flexibly with a wide range of problems. Some general characteristics of GA are shown in the Appendix (Section 8.3). The main steps of the developed GA-based bicriterion optimisation program for electrified railways are as follows.

#### 4.1 Encoding and decoding

When GAs are used to solve an optimisation problem it is necessary to represent the solution in a string form. The process is called encoding. Standard genetic operators, crossover and mutation, are operated on the string to search for optimal solutions. The technique for encoding solutions may vary from problem to problem. Generally, the binary encoding method is used, and is also adopted in this work. In addition, it is necessary to decode each string into the corresponding decimal value when the solution process terminates.

Each candidate solution ( $\beta_j, j = 1, 2, \dots, N_{TSS}$ ) is represented by a binary string as

$$\text{string:} \left| \text{xxxxxxxxxx} \right| \left| \text{xxxxxxxxxx} \right| \dots \left| \text{xxxxxxxxxx} \right| \\ \leftarrow \beta_1^{(2)} \quad \rightarrow \leftarrow \beta_2^{(2)} \quad \rightarrow \quad \leftarrow \beta_{N_{TSS}}^{(2)} \quad \rightarrow \quad (9)$$

The superscript '2' denotes a binary number. This means that value of  $j$ th TSS firing angle is represented by  $\beta_j^{(2)}$  ( $j = 1, 2, \dots, N_{TSS}$ ), which is a 10-bit binary number. Such a length is chosen to achieve trade-off between the computing expense and precision requirements. Thus two binary strings 0000000000 and 1111111111 are used to represent the corresponding binary values of  $\beta_j^{\min}$  and  $\beta_j^{\max}$ , respectively, and the binary value corresponding to  $\beta_j$  ( $j = 1, 2, \dots, N_{TSS}$ ) is mapped linearly in between. The precision of this mapping coding is calculated using

$$(\beta_j^{\max} - \beta_j^{\min}) / (2^{10} - 1) \quad (10)$$

where  $j$  represents a TSS, which can either be in rectifying mode or in inverting mode. Thus the value of  $j$ th firing angle  $\beta_j$  can be derived from  $\beta_j^{(10)}$ , where  $\beta_j^{(10)}$  is a decimal number converted from  $\beta_j^{(2)}$

$$\beta_j = \beta_j^{\min} + \beta_j^{(10)} (\beta_j^{\max} - \beta_j^{\min}) / (2^{10} - 1) \quad (11)$$

This is called the decoding process.

#### 4.2 Principal modules of GA-based optimisation

The developed program is implemented using object-oriented techniques on PC-compatible, and contains five principal modules for initialisation, constraint, evaluation, selection and recombination.

The initialisation module is used to create initial candidate solutions. The constraint module checks if each candidate solution satisfies the required constraints. The evaluation module uses a fitness function to assess the goodness of each candidate solution to the problem to be solved. The selection module involves selecting a

specified number of solutions for breeding. The recombination module is in charge of manipulating the current population and creating new candidate solutions via reproduction. Implementation details of the developed GA-based bicriterion optimisation program are as follows.

**4.2.1 Initialisation module:** This is to produce the initial candidate solutions randomly. A candidate solution is produced using a random number generator. Afterwards, the candidate is mapped into the allowable range of each substation  $k$ ,  $[\beta_k^{\min}, \beta_k^{\max}]$ ,  $k = 1, 2, \dots, N_{TSS}$ , where substation  $k$  can either be on rectifying mode or inverting mode. The process is repeated until the number of the candidate solutions in the population equals the specified population size  $N_p$ .

**4.2.2 Constraint module:** This checks whether each candidate solution satisfies all constraints. At first, AC/DC loadflow is run to check the feasibility of each candidate solution with respect to the constraints. If it is feasible it is placed in the current population, otherwise it is discarded.

**4.2.3 Evaluation module:** This evaluates the fitness of each candidate solution in the current population. Only those candidates satisfying all constraints are evaluated and are then ranked in order of decreasing fitness. Generally, the problem to be solved is required to be a maximisation problem. So the objective function of eqn. 3 which is minimised is transformed into the following fitness function:

$$\text{Fit}(\bar{\beta}) = \frac{c1}{\rho \cdot \text{Obj}1(\bar{\beta}) + (1 - \rho) \cdot \text{Obj}2(\bar{\beta}) + \rho \cdot c2} \quad (12)$$

where  $c1$  is a specified *fitness scaling* constant that is used to map the fitness value into a preferable domain.  $c2$  is a constant which is used to guarantee positive values of  $\text{Fit}(\bar{\beta})$  and  $\text{Obj}1(\bar{\beta}) + c2$ . The meaning of other symbols is the same as that in eqn. 3. Typical values of  $c1$  and  $c2$  are  $10^6$  and  $16 \times 10^6$  against the maximum power recovery of 15.39MW, respectively.

**4.2.4 Selection module:** This selects a specified number of candidate solutions of high fitness for breeding. In this work, the commonly used roulette wheel selection is adopted [13, 14]. The probability for each parent to be selected is directly proportional to its fitness, i.e. the candidate with a higher fitness value has a higher opportunity to reproduce the next new population.

**4.2.5 Recombination module:** This is a process of producing new candidate solutions from the old population. Two operators are adopted for recombination, i.e. crossover and mutation. In addition, elitism strategy is implemented as a technique to ensure survival of the fittest candidate solutions in each population. This is achieved by copying the best members of each generation into the succeeding generation. Moreover, if more than one candidate solution are the same in the current population, then only one of them is retained so as to prevent the super candidate solutions from occurring. At the end a new generation of candidate solutions is formed whose size remains to be  $N_p$ . This is an iterative process, and average fitness of the candidate solution can be increased from generation to generation.

## 5 Test results and analysis

A typical MRT system is used for testing the feasibility and efficiency of the developed method. The rectifier configuration is the standard parallel 12-pulse. It possesses low harmonic distortion of alternating line current and direct voltage, together with an acceptable structure complexity and cost. Rectifiers are normally equipped with diodes and are incapable of voltage regulation. Inverters are equipped with thyristor bridges.

The test system is a typical two-track railway line with an overall length of 19.833km, 14 passenger stations and seven TSSs (four of them with inverters). Each TSS is energised from a 66kV distribution line and supplies power to trains at a nominal DC third-rail voltage of 750V. Trains are equipped with a continuous blending of regenerative and rheostatic braking. Each DC line is represented by a resistance value of  $0.009\Omega/\text{km}$ . Resistance of each TSS is  $0.006\Omega$  in inverting mode and  $0.01\Omega$  in rectifying mode, respectively. Other data of the study system are attached in the Appendix (Section 8.2, Tables 1 and 2).

GA parameters are typically specified as  $N_p = 400$  and  $MG = 50$ . Other parameters are given in the Appendix (Section 8.3). Optimisations have been conducted for many operating conditions, but only one test case at a particular time is described here. At such a simulation time, seven trains are braking and seven trains are motoring. Since there is power surplus in the railway system, all four of the TSSs equipped with inverters are inverting. Positions and consumptions of the 14 trains are listed in the Appendix (Section 8.2, Table 2). Figs. 4-9 illustrate the optimisation results, whose salient points follow.

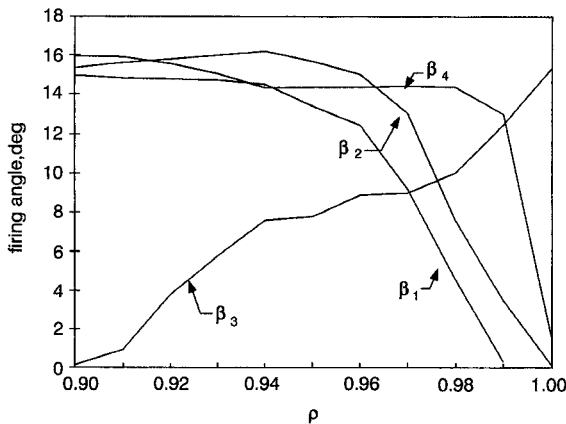


Fig. 4 Firing angle of converter as function of objective weight

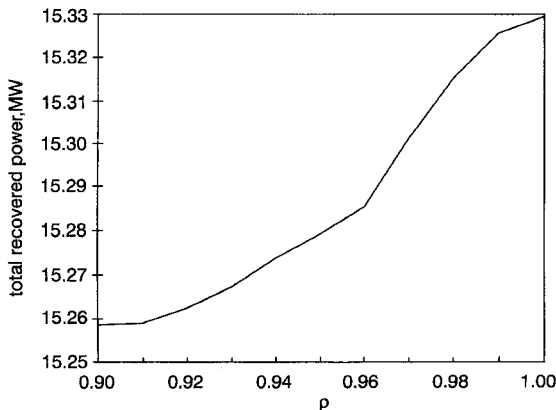


Fig. 5 Total recovered power as function of objective weight

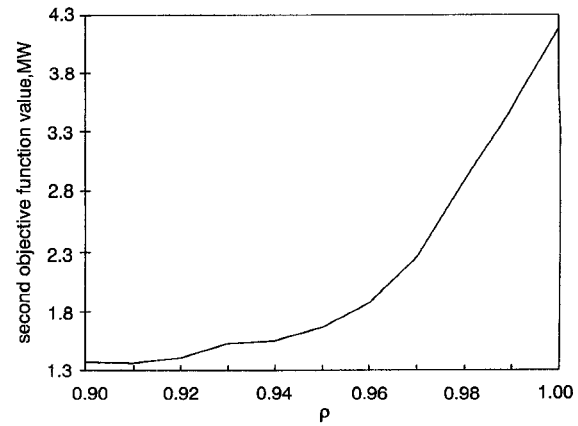


Fig. 6 Second objective function as function of objective weight

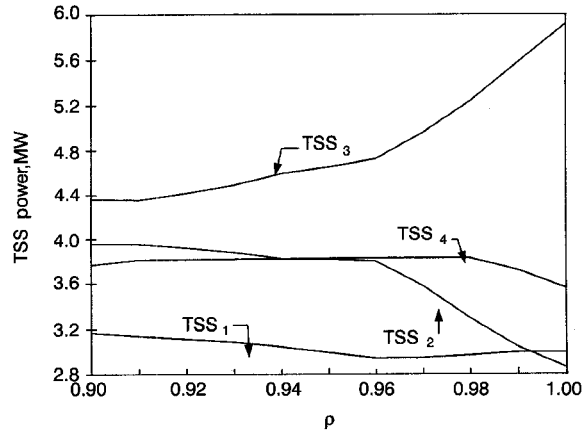


Fig. 7 TSS load as function of objective weight

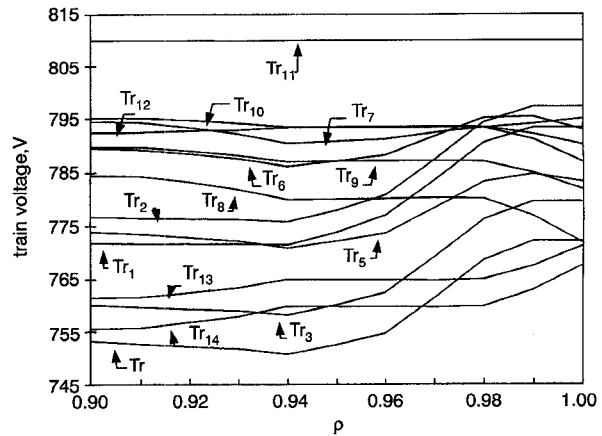


Fig. 8 Train voltage as function of objective weight

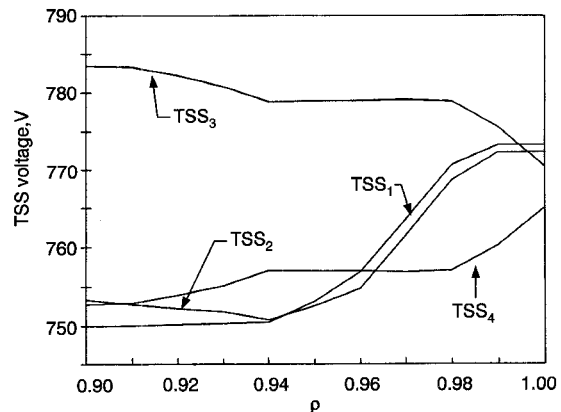


Fig. 9 TSS voltage as function of objective weight

(a) Fig. 4 shows the optimal TSS firing angles  $\beta_k$ ,  $k = 1, 2, 3, 4$  over a range of  $\rho = 0.9 \sim 1$ .

(b) Over this  $\rho$ -range, the total recovered power by all TSSs ( $Obj1(\bar{B})$ , Fig. 5) and the recovered power by each TSS (Fig. 7) are approximately proportional to  $\rho$ . In contrast, load sharing among TSSs ( $Obj2(\bar{\beta})$ , Fig. 6) is roughly inversely proportional to  $\rho$ . This is because in this  $\rho$ -range, great emphasis is placed to increase power returned by all TSSs. When  $\rho = 1$ , only the first objective is considered and the total recovered power reaches its maximum value, corresponding to a power saving of 6.2%.

(c) Figs. 4–9 have not included results in the range of  $\rho = 0 \sim 0.9$ . In this range the total recovered power, recovered power by each TSS, and load sharing are all quite insensitive to  $\rho$ -values.

(d) Figs. 8 and 9 show the voltage performance for each train and for each TSS. Without TSS firing-angle optimisation, train voltages have risen to a maximum value of 827.41 V that is well above the design upper limit of 810 V. Rheostatic braking has been activated to remove such overvoltages. As a result, regenerated power has not been fully recovered. With TSS firing-angle optimisation, all train voltages have been kept within the permitted limits between 600 V and 810 V for all  $\rho$ -values (Figs. 8 and 9). In general, the proposed method has achieved a better direct voltage profile. Compared with the first objective the total power reduction objective achieves a higher power recovery (Fig. 6,  $\rho = 1$ ) as prescribed, a better voltage profile (Figs. 5, 8 and 9,  $\rho = 1$ ), but a much inferior load sharing (Fig. 7,  $\rho = 1$ ) among the TSSs.

Test results confirm that both the objectives have significantly been improved by optimising TSS firing angles using the proposed algorithm. Tradeoff curves as in Figs. 4–9 are obtained with only railway network constraints included in optimisation. To include other feasibility and quality considerations, these tradeoff curves can be used for compromising global optima with local optima or suboptima. The use of fuzzy performance indices for representing feasibility and quality considerations was well documented [6]. Application of the techniques in this area will be reported later.

## 6 Conclusions

The paper has developed a bicriterion optimisation model and a GA-based method to optimal co-ordination control of TSS firing angles. A mechanism is developed for compromising power recovery with load sharing. With performance curves plotted with a full range of  $\rho$ -values, a basis for making tradeoffs is formed between the two objectives. Simulation results have shown that the developed mathematical model is feasible, and the proposed GA-based method is mathematically exact and efficient. Consistent power saving has been observed from the simulation results, and load sharing can be greatly improved through co-ordinated optimisation of TSS firing angles. The optimisation in this paper was carried out at a particular 'snap shot' in time. The proposed approach is being extended to a period of time for dealing with energy recovery.

## 7 References

- 1 WINDLE, C.J.: 'Energy saving strategies employed on the Singapore MRT'. Proceedings of international conference on *Mass rapid transit worldwide*, Institute of Engineers, Singapore, 1986, pp. 397–404
- 2 MELLITT, B., MOUNEIMNE, Z.S., and GOODMAN, C.J.: 'Simulation study of DC transit systems with inverting substation', *IEE Proc. B*, 1984, **131**, (2), pp. 38–50
- 3 OLG, E., IKEDA, M., TAMURA, K., and TANAKA, S.: 'Railway substation system with regenerative inverter', *Hitachi Rev.*, 1986, **35**, (6), pp. 323–328
- 4 SUZUKI, T.: 'DC power-supply system with inverting substations for traction systems using regenerative brakes', *IEE Proc. B*, 1982, pp. 18–26
- 5 MELLITT, B., SUJITJORN, S., GOODMAN, C.J., and RAMBUKWELLA, N.B.: 'Energy minimisation using an expert system for dynamic coast control in rapid transit trains'. Proceedings of international conference on *Railway engineering*, Institution Engineers, Perth, Australia, 1987, pp. 48–52
- 6 CHANG, C.S., PHOA, Y.H., WANG, W., and THIA, B.S.: 'Economy/regularity fuzzy-logic control of DC railway systems using an event-driven approach', *IEE Proc., Electr. Power Appl.*, 1996, **143**, (1), pp. 9–17
- 7 MELLITT, B., GOODMAN, C.J., and ARTHURTON, R.I.M.: 'Simulation studies of energy saving with chopper control on the Jubilee Line', *IEE Proc. B*, 1978, **125**, (4), pp. 304–310
- 8 MELLITT, B., GOODMAN, C.J., and ARTHURTON, R.I.M.: 'Simulator for studying operational and power-supply conditions in rapid-transit railways', *IEE Proc. B*, 1978, **125**, (4), pp. 298–303
- 9 FIRPO, P., and SAVIO, S.: 'Optimal control strategies for energy management in Metrorail transit systems'. Proceedings of 4th international conference on *Computer aided design, manufacture and operation in railway and other advance mass transit systems*, Madrid, 1994, (Computational Mechanics Publications, Spain), Vol. 2, pp. 387–394
- 10 XU, J.X., CHANG, C.S., and WANG, X.W.: 'Constrained multi-objective global optimisation of longitudinal interconnected power system by genetic algorithm', *IEE Proc., Gener. Transm. Distrib.*, 1996, **143**, (5), pp. 435–446
- 11 CHANG, C.S., and THIA, B.S.: 'Online rescheduling of mass rapid transit systems: fuzzy expert system approach', *IEE Proc., Electr. Power Appl.*, 1996, **143**, (4), pp. 307–316
- 12 CHANG, C.S., CHAN, T.T., HO, S.L., and LEE, K.K.: 'AI applications and solution techniques for AC railway system control and simulation', *IEE Proc. B*, 1993, **140**, (3), pp. 166–176
- 13 GOLDBERG, D.E.: 'Genetic algorithms in search, optimization, and machine learning' (Addison-Wesley, 1989)
- 14 DAVIS, L.: 'Handbook of genetic algorithms' (Van Nostrand Reinhold, NY, 1991)

## 8 Appendix

### 8.1 AC/DC loadflow algorithm

A method of successive displacements is used. AC loadflow and DC loadflow are executed separately and sequentially [6]. Both AC and DC loadflows are iterative, because they are both formulated in nonlinear equations. For AC loadflow, the fast decoupled method is used and sparsity techniques are exploited. The implemented DC loadflow program deals with the following factors encountered in DC electrified railway simulation.

**8.1.1 DC loadflow:** The network equation of the DC system is

$$I_d = GV_d \quad (13)$$

where  $I_d$  is a vector of busbar injected currents which can either be a train current, a rectifier output, or an inverter input (Fig. 10).  $V_d$  is a vector of train terminal or busbar voltages.  $G$  is the nodal conductance matrix of the DC system. Train injected currents are derived from typical train consumption – distance plot which may either be of constant-power characteristic

$$I_{tr} = P_{tr}^{sp}/V_{tr} \quad (14)$$

or of the constant-current characteristic

$$I_{tr} = I_{tr}^{sp} \quad (15)$$

where  $I_{tr}$ ,  $P_{tr}$  and  $V_{tr}$  are each train's injected current, power consumption and terminal voltage, respectively.

Superscript 'sp' stands for a specified or known quantity. A powerful method [12] was developed to refer all train currents to their nearest busbars and/or traction stations, and thus eliminate all trains from the network equation. This so-called 'train load referral' process maintains the structure of nodal conductance matrix  $G$  which needs to be reconfigured and inverted once only unless there is a change of railway network configuration.

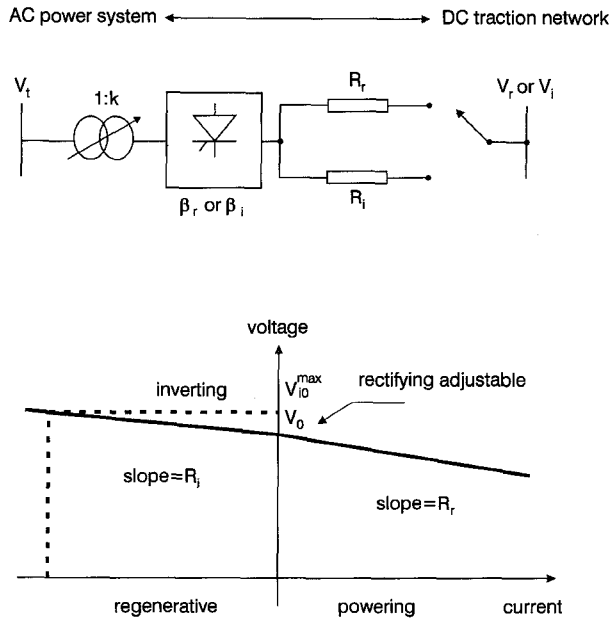


Fig. 10 Traction station model and characteristics

By inserting high-resistance links, the structure of  $G$  is preserved after each temporary change or switching operation. Mode changes of rectifier/inverter stations are modelled by varying shunt branches attached to the respective busbars (Fig. 10). Such changes are incorporated into the inverse of matrix  $G^{-1}$  using a technique such as the matrix inversion lemma [12].

Since train consumptions are either constant-power or constant-current (eqns. 14 and 15), the DC network solution takes the following steps of successive voltage displacements:

- (i) Using all constant-power train consumptions, obtain the first voltage displacement  $\Delta V_d^{(1)}$  by iteratively solving eqn. 14
- (ii) Using all constant-current train consumptions, obtain the second voltage displacement  $\Delta V_d^{(2)}$  by directly solving eqn. 15
- (iii) Update all direct voltages by superimposing  $\Delta V_d^{(1)}$  and  $\Delta V_d^{(2)}$  onto the initial voltages  $V_d^{(0)}$ .

Having obtained the network solution one then uses interpolation [12] to evaluate voltages across each train using voltages of the nearest fixed buses. Should there be any overvoltage detected in the loadflow results, rheostatic braking is progressively blended to remove these overvoltages. Braking currents are reduced, and eqns. 13–15 are resolved.

**8.1.2 AC loadflow:** The standard method of fast decoupled loadflow with sparsity technique [6] has been used. AC sources are represented by an equivalent current source and reactance for the grid's short-circuit MVA. Tap-changing transformers and power-factor compensation devices have also been modelled.

### 8.1.3 Combined solution of DC/AC loadflow:

The basic algorithm modifies the AC network status using results from DC loadflow. For each traction station the active and reactive power mismatches are

$$\begin{aligned} \Delta P_i &= P_i^{sp} - P_i^{ac} - P_i^{dc} \\ \Delta Q_i &= Q_i^{sp} - Q_i^{ac} - Q_i^{dc} \end{aligned} \quad (16)$$

where  $P$  and  $Q$  represent the bus active and reactive powers. Superscripts 'ac' and 'dc' represent the AC and DC quantities, respectively. Active and reactive power supplied to the DC side of each traction station are given by [6]

$$\begin{aligned} P_i^{dc} &= k_1 a V_i I_i \cos \phi \\ Q_i^{dc} &= k_1 a V_i I_i \sin \phi \end{aligned} \quad (17)$$

where  $a$ ,  $V_i$ ,  $I_i$ ,  $\phi$  and  $k_1$  are, respectively, the transformer off-nominal turns ratio, rectifier or inverter terminal voltage, station injected current, power factor angle, and a constant associated with a certain rectifier/inverter configuration.

## 8.2 Study network data about TSSs

See Tables 1 and 2.

Table 1: Information about the traction stations

Train no.	Position (m)	Type	$V_{r0}$ (V)	$R_r$ ( $\Omega$ )	$V_i$ (V)	$R_i$ ( $\Omega$ )
0	0	3	750	0.01	750	0.006
1	1021	0	750	0.01	750	0.006
2	2013	1	750	0.01	750	0.006
3	2806	0	750	0.01	750	0.006
4	3842	3	750	0.01	750	0.006
5	5088	0	750	0.01	750	0.006
6	6243	1	750	0.01	750	0.006
7	7704	0	750	0.01	750	0.006
8	8595	3	750	0.01	750	0.006
9	9772	0	750	0.01	750	0.006
10	12126	1	750	0.01	750	0.006
11	13558	0	750	0.01	750	0.006
12	18485	3	750	0.01	750	0.006
13	19833	0	750	0.01	750	0.006

$V_{TSS_k}^{min} = 750V$ ,  $V_{TSS_k}^{max} = 801V$ ,  $k = 1, 2, 3, 4$ ;  $V_{r0} = 750V$ ;  $V_{i0} = 750V$ ;  $R_{r0} = 0.01\Omega$ ;  $R_{i0} = 0.006\Omega$ ;  $V_{TSS_j}^{min} = 600V$ ,  $V_{TSS_j}^{max} = 810V$ ,  $j = 1, 2, \dots, 14$

Nominal track voltage: 750V

Nominal track resistance: 0.009 $\Omega$ /km

TSS type: 0  $\rightarrow$  off

1  $\rightarrow$  TSS with rectifiers only

3  $\rightarrow$  TSS with rectifiers and inverters

## 8.3 General characteristics of genetic algorithm

GAs [13, 14] are search procedures whose mechanics are based on those of natural genetics. Many different forms of GA have been proposed. Some points associated with the GA used in this work are described as follows:

(a) There are many methods to select two parents from the old population, and different GA methods can be obtained by using different selection methods. In the paper, the roulette wheel selection is employed [13, 14].

(b) Crossover is the most important operator in GA, and it is applied with the probability  $P_c$  which is typically between 0.6 and 0.9. The crossover operator

**Table 2: Train positions and consumptions at time of optimisation**

Train no.	Position (m)	Consumption (kW)
1	1099.5	-2321.6
2	1902.1	-2985.2
3	3146.1	225.0
4	3842.0	450.0
5	5281.6	225.0
6	6165.7	-2297.7
7	7799.3	-2665.9
8	8551.4	-1607.9
9	10621.1	225.0
10	11703.6	225.0
11	13687.4	-3363.5
12	14664.7	225.0
13	17482.2	225.0
14	18407.5	-2301.1

takes two strings from an old population and exchanges some contiguous segment of their structures to form two offsprings. Either the single-point

crossover, two-point crossover operator or uniform crossover operator [14] may be used.

(c) Mutation is also an important operator of GA. In a binary encoded GA, the mutation operator randomly switches one or more bits with some small probability  $P_m$  which is typically between 0.001 and 0.01.

(d) Both  $P_c$  and  $P_m$  may be entered at the beginning of the program, and maintained constant throughout the entire GA run. Alternatively,  $P_c$  and  $P_m$  may be changed from generation to generation according to the following equations:

$$P_c^{(t)} = P_c^{(t-1)} - [P_c^{(0)} - 0.6]/MG \quad (18)$$

$$P_m^{(t)} = P_m^{(t-1)} + [0.1 - P_m^{(0)}]/MG \quad (19)$$

where  $MG$  is the number of maximum generations allowed, and  $t$  denotes the present generation.  $P_c^{(0)}$  and  $P_m^{(0)}$  denote initial values of crossover and mutation probabilities, respectively.  $P_c^{(t)}$  and  $P_m^{(t)}$  denote crossover and mutation probabilities at  $t$ th generation, respectively. Different schemes of crossover and mutation operators have been experimented. In this work  $P_c^{(0)}$  and  $P_m^{(0)}$  in eqns. 18 and 19 are set to be 0.9 and 0.001, respectively.